Exclusive Z^0 production in ep and eA collisions at high energies

G. M. Peccini[*] and M. V. T. Machado[†]

High Energy Physics Phenomenology Group, GFPAE. Universidade Federal do Rio Grande do Sul (UFRGS) Caixa Postal 15051, CEP 91501-970, Porto Alegre, RS, Brazil

L. S. Moriggi[‡]

Universidade Estadual do Centro-Oeste (UNICENTRO), CEP 85040-167 Guarapuava, PR, Brazil

(Received 25 April 2022; accepted 25 June 2022; published 5 July 2022)

In this work the $k_\perp$-factorization formalism is applied to compute the exclusive Z^0 boson photoproduction in ep and eA collisions. The study is also extended to pp and AA processes. The nuclear effects are investigated considering heavy and light ions. Analytical models for the unintegrated gluon distribution are taken into account and the corresponding theoretical uncertainty is quantified. The analysis is done for electron-ion collisions at the Large Hadron-Electron Collider, its high-energy upgrade and at the Future Circular Collider in lepton-hadron mode. Additionally, ultra-peripheral heavy ion collisions at future runs of the Large Hadron Collider and at the Future Circular Collider (hadron-hadron mode) are also considered.

DOI: 10.1103/PhysRevD.106.014002

I. INTRODUCTION

The Large Hadron Collider (LHC) has studied physics at TeV scale allowing the access to unexplored kinematical regimes at large luminosities. This machine is able to search and study the physics beyond of the Standard Model (SM) with high accuracy. Traditionally, a baseline SM signal is the Z^0 production [1]. In proton-proton (pp) collisions, the hadronic Z^0 decays are not easy to identify due to the strong background of QCD multijet production from hadronic event environment [2]. The high-statistics measurements in final states with leptons are the main channel at the LHC. On the other hand, the exclusive production of Z^0 at electron-ion colliders or in ultraperipheral collisions (UPCs) present some advantages. There is an increasing interest on exclusive processes at the LHC. [3,4]. One of these favorable conditions is the processes to be perturbatively calculable with not so large uncertainties due to the high mass of the boson. Another feature is the clear experimental signature compared to the Z^0 signal coming from hadroproduction. A dedicated experimental search has already been done for $p\bar{p}$ collisions at the Tevatron [5]. No exclusive $Z \to \ell^+\ell^-$ candidates were observed leading to the first upper limit on the exclusive Z^0 cross section, $\sigma(p\bar{p} \to pZ^0\bar{p}) < 0.96$ pb. Similar searches have been preliminarily carried out at the LHC [6]. Therefore, it is timely to investigate the prediction for both electron-ion colliders and ultraperipheral collisions given their high energies and integrated luminosities [see Ref. [7] where prospects for exclusive processes which are complementary between the LHC and the Electron-Ion Collider (EIC) are discussed].

The exclusive Z^0 photoproduction in electron-proton collisions was first addressed in the pioneering work of Ref. [8], where an analysis using nonforward QCD planar ladder diagrams was done and applied to diffractive (inclusive and semi-inclusive) boson production in ep colliders. The simple two-gluon exchange model of the Pomeron was used in Ref. [9] to compute the boson photoproduction cross section. There, a finite gluon mass has been included in the propagators to suppress the long distance contributions. In the context of the color dipole picture, the exclusive Z^0 production has been analysed in both spacelike [10] and timelike kinematics [11]. The equivalent calculation in $k_\perp$-factorization approach was presented first in Ref. [12]. In Refs. [11,12], applications to photoproduction in pp collisions at the LHC energies were performed. The analysis for UPCs in pp, pA, and AA collisions at the LHC has been done in Ref. [13].

In this paper, the main goal is to compute the exclusive Z_0 production cross section in ep and eA collisions by using the $k_\perp$-factorization formalism. Different models for the unintegrated gluon distribution (UGDs), $\mathcal{F}(x, k_\perp^2)$, will

[*]guilherme.peccini@ufrgs.br
[†]magnus@if.ufrgs.br
[‡]lucasmoriggi@unicentro.br

Published by the American Physical Society under the terms of the Creative Commons Attribution 4.0 International license. Further distribution of this work must maintain attribution to the author(s) and the published article's title, journal citation, and DOI. Funded by SCOAP[3].

be considered. We focus on the energies and phase space of the Large Electron-Hadron Collider (LHeC) [14–16] and the Future Circular Collider (FCC) [17,18] in eh mode (FCC-eh). Using the obtained cross section for Z^0 production in photon-proton and photon-nucleus processes, the corresponding predictions for pp and AA collisions are computed. In the last case, the cross section at the energies of the High Luminosity LHC (HL-LHC), High Energy LHC (HE-LHC), and FCC are calculated. The sources of theoretical uncertainties are investigated. An important point to be highlighted is that this present paper extends our previous works on the exclusive dilepton production in lepton-hadron and hadron-hadron machines [19,20]. This work is organized as follows. In Sec. II, the theoretical formalism for ep (Sec. II A) and eA collisions (Sec. II B) is briefly reviewed along with the calculations concerning the analytical models for UGDs in proton and nuclei. In Sec. III, the numerical results are presented for the energies relevant to the LHeC machine. The number of events per year is obtained without imposing any further kinematic cuts. In addition, the cross section for photoproduction in pp collisions and in AA UPCs are studied using the equivalent photon approximation. A comprehensive analysis is performed for light nuclei and lead as well. In the last section, we summarize the results and present the main conclusions.

II. THEORETICAL FORMALISM

A. Exclusive Z^0 production in electron-proton collisions

The calculation of exclusive Z^0 production cross section follows the same formalism of TCS (timelike Compton scattering) [19–21]. In the context of the k_T-factorization approach it was first proposed in Ref. [12] using only one model for the UGD. Afterwards, in Ref. [19] the present authors computed the TCS cross section for dilepton production in ep collisions by using different and updated UGDs. Specifically, four UGDs containing distinct physical information were analyzed. Moreover, in Ref. [20] we have accounted for dilepton production via TCS in electron-nucleus collisions assuming the UGD proposed in Ref. [22] [referred to as the MPM (Moriggi-Peccini-Machado) model hereafter]. In the present work, we will consider the same UGDs utilized in Ref. [19] to evaluate the cross section for exclusive Z^0 production.

Comparing to TCS, one can calculate the cross section for exclusive Z^0 boson production by simply replacing the electromagnetic photon-quark coupling by the electroweak one, $ee_f \to \frac{eg_V^f}{\sin 2\theta_W}$, where θ_W is the Weinberg angle. Only the weak vector coupling is relevant, where $g_V^f = (I_3^f - 2e_f \sin^2\theta_W)/\sin 2\theta_W)$ [11]. The weak isospin of a quark of flavor f and charge ee_f is I_3^f. Along with the coupling replacement, one has also to redefine x in terms of the Z^0 mass,

$$x = \xi_{\rm sk}\left(\frac{M_Z^2}{W^2}\right), \tag{1}$$

where $\xi_{\rm sk}$ is inserted in order to correct the skewedness effect [21]. Following Ref. [12], the value $\xi_{\rm sk} = 0.41$ has been considered.

Taking the equation for the imaginary part of TCS amplitude expressed in Refs. [19–21] and performing the coupling replacement, one can obtain the forward amplitude for exclusive Z^0 production in ep collisions [12]:

$$\mathcal{M}(W, |t| = 0) = \sum_f \frac{2W^2\alpha_{em}g_V^f}{\pi}\int_0^1 dz \int d^2\vec{\kappa}_\perp \frac{(i+\rho_R){\rm Im}A_f(z,\vec{\kappa}_\perp)}{\kappa_\perp^2 + m_f^2 - z(1-z)M_Z^2 - i\varepsilon}, \tag{2}$$

where ρ_R is the ratio of real to imaginary part of amplitude. Moreover, m_f is the quark mass of flavor f and W^2 is the center-of-mass energy squared of the photon-proton system. The quantity ${\rm Im}A_f$ is defined as

$${\rm Im}A_f(z,\vec{\kappa}_\perp) = \int \frac{\pi dk_\perp^2}{k_\perp^4}\alpha_s(\mu^2)\mathcal{F}(x,k_\perp^2)C(z,\kappa_\perp,k_\perp,m_f),$$

where the explicit expression for the function $C(z,\kappa_\perp,k_\perp, m_f)$ can be found in Refs. [12,19]. The following hard scale $\mu^2 = \max(\kappa_\perp^2 + m_f^2, k_\perp^2)$ has been chosen. The corresponding amplitude for the $\gamma p \to Z^0 p$ process within the diffraction cone is written as

$$\mathcal{M}(W,|t|) = \mathcal{M}(W,|t|=0)e^{-B_D|t|}, \tag{3}$$

where the energy dependent diffraction slope, B_D, is parametrized as $B_D = B_0 + 2\alpha'_{\rm eff}\log(W^2/W_0^2)$. Here, $\alpha'_{\rm eff} = 0.164\ {\rm GeV}^{-2}$, $B_0 = 3.5\ {\rm GeV}^{-2}$, and $W_0 = 95$ GeV [12].

The differential and the integrated production cross section are, respectively, given by

$$\frac{d\sigma}{dt}(\gamma p \to Z^0 p) = \frac{|\mathcal{M}(W,|t|)|^2}{16\pi}, \tag{4}$$

$$\sigma(\gamma p \to Z^0 p) = \frac{[{\rm Im}(\mathcal{M}^{\gamma p \to Z^0 p})]^2(1+\rho_R^2)}{16\pi B_D}, \tag{5}$$

The cross section in Eq. (5) will be evaluated for the LHeC (as well for its high luminosity and high energy upgrades) [14–16,23] and for the FCC center-of-mass energies [17,18]. These energies are summarized in Table I. Concerning the quark flavors, u, d, s, c, b are considered.

For the numerical calculation, three models for the UGD will be taken into consideration: the MPM [24], Ivanov-Nikolaev (IN) [25], and Golec-Biernat-Wusthoff (GBW) [26,27] models. The MPM and GBW models are

TABLE I. Energies of the beams at future electron-proton colliders (LHeC/HL-LHeC, HE-LHeC, and FCC-eh).

Collider	E_e (GeV)	E_p (TeV)	$\sqrt{s}$ (TeV)
LHeC/HL-LHeC	60	7	1.3
HE-LHeC	60	13.5	1.7
FCC-eh	60	50	3.5

analytical, whereas IN is dependent on the input for the Dokshitzer–Gribov–Lipatov–Altarelli–Parisi (DGLAP) evolved gluon distribution. The first one present also the geometric scaling property, i.e., the UGD depends on the scaling function $\tau_s = k_\perp^2/Q_{sp}^2(x)$. The proton saturation scale in this case scales on x in the form $Q_{sp}^2 = (x_0/x)^\lambda$. The three models are parametrized as follows:

$$\mathcal{F}_{\rm MPM}(x,k_\perp^2) = k_\perp^2 \frac{3\sigma_0}{4\pi^2\alpha_s}\frac{(1+\delta n)\tau_s}{(1+\tau_s)^{2+\delta n}}, \tag{6}$$

$$\mathcal{F}_{\rm GBW}(x,k_\perp^2) = k_\perp^2 \frac{3\sigma_0}{4\pi^2\alpha_s}\tau_s e^{-\tau_s}, \tag{7}$$

$$\mathcal{F}_{\rm IN}(x,k_\perp^2) = \mathcal{F}_{\rm soft}^{(B)}(x,k_\perp^2)\frac{\kappa_s^2}{k_\perp^2+\kappa_s^2} + \mathcal{F}_{\rm hard}(x,k_\perp^2)\frac{k_\perp^2}{k_\perp^2+\kappa_h^2}. \tag{8}$$

In the MPM, one has $\delta n = a\tau^b$ and $Q_s^2 = (x_0/x)^{0.33}$ (here, $\lambda = 0.33$ value is fixed), where the parameters σ_0, x_0, a, and b were fitted against DIS data in the kinematic domain $x < 0.01$ [24]. A fixed value $\alpha_s = 0.2$ has been considered. Beside describing DIS data at small x, it also describes the spectra of produced hadrons in pp and $p\bar{p}$ processes. This model was built by means of the geometric scaling approach and a Tsallis-like behavior of the measured spectra. For the GBW parametrization, the updated parameters σ_0, x_0, and λ (fit including bottom quark contribution) are taken from Ref. [27]. Concerning the IN model, the functions $\mathcal{F}_{\rm sof}^{(B)}$ and $\mathcal{F}_{\rm hard}$ as well as the quantities $\kappa_{s,h}$ can be found in Ref. [25].

In what follows, we will perform the extension of the above approach to eA collisions. The dependence on energy and atomic number is addressed as well as the estimation of the theoretical uncertainty.

B. Exclusive Z^0 production in electron-nucleus collisions

In case of electron-nucleus collisions, the main difference from electron-proton collisions is the unintegrated gluon distribution. Accordingly, we will utilize a nuclear UGD instead of a proton UGD here. The nuclear UGD considered will be obtained by applying the Glauber-Mueller formalism. Additionally, one has to take into account the nuclear form factor, $F_A(q)$. In this work, an analytic form factor given by a hard sphere of radius $R_A = 1.2A^{1/3}$ fm, convoluted with a Yukawa potential with range $a = 0.7$ fm, has been considered [28]. Therefore, the differential cross section for eA collisions is given by

$$\frac{d\sigma}{dt}(\gamma A \to Z^0 A) = \frac{[{\rm Im}(\mathcal{M}^{\gamma A\to Z^0 p})]^2((1+\rho_R^2)}{16\pi}|F_A(q)|^2, \tag{9}$$

$$F_A(q) = \frac{4\pi\rho_0}{A|q^3|}\left(\frac{1}{1+a^2q^2}\right)[\sin(qR_A) - qR_A\cos(qR_A)], \tag{10}$$

where $q = \sqrt{|t|}$. Namely, the amplitude depends on t in a factorized way, $\mathcal{M}(W^2,t) = \mathcal{M}(W^2,t=0)F_A(q)$.

For Z^0 production in nuclear collisions, we will investigate the nuclei proposed in the LHC prospects (see Refs. [29–31]), namely O, Kr, Ar, and Pb. The energy of the nuclear beams are given by the energy of the proton beam multiplied by the ratio Z/A, where Z is the atomic number while A is the atomic mass number. In Table II, we outline the beam energies along with the center-of-mass energies for electron-nucleus collisions. The energy of the electron beam is 60 GeV.

As stressed out previously, the nuclear unintegrated gluon distribution is in order rather than the proton one to compute the amplitude in Eq. (2). In this context, in Ref. [22] the MPM model was adapted to nuclear targets by using Glauber-Gribov formalism [32,33], leading to the following form for the nuclear UGD:

$$\mathcal{F}_A(x,k_\perp^2,b) = k_\perp^2\frac{3}{4\pi^2\alpha_s}k_\perp^2\nabla_{k_\perp}^2\mathcal{H}_0\left\{\frac{1-S_{\rm dip}^A(x,r,b)}{r^2}\right\}, \tag{11}$$

where $\mathcal{H}_0\{f(r)\} = \int drrJ_0(k_\perp r)f(r)$ is the order zero Hankel transform and the quantity $S_{\rm dip}^A$ is given by [34]

$$S_{\rm dip}^A(x,r,b) = {\rm e}^{-\frac{1}{2}T_A(b)\sigma_{\rm dip}(x,r)}. \tag{12}$$

Here, $\sigma_{\rm dip}(x,r)$ is the dipole cross section for the proton case. The function $T_A(b)$ is the thickness function and depends on the impact parameter, b, and normalization

TABLE II. Center-of-mass energies (in units of TeV) at future electron-nucleus colliders (LHeC/HL-LHeC, HE-LHeC, and FCC-eA) for different nuclei.

Nucleus	LHeC/HL-LHeC	HE-LHeC	FCC-eA
O	0.92	1.27	2.45
Ar	0.87	1.21	2.32
Kr	0.85	1.18	2.27
Pb	0.81	1.13	2.18

$\int d^2bT_A(b) = A$. A Woods-Saxon parametrization for the nuclear density [35] has been considered.

In case of a proton target, a homogeneous object with radius R_p is assumed which factorizes $S_{\rm dip}(x,r,b)$ into $S_{\rm dip}(x,r,b) = S_{dp}(x,r)\Theta(R_p - b)$. For large dipoles, $S_{\rm dip}(x,r) \to 0$ and the cross section reaches a bound given by $\sigma_0 = 2\pi R_p^2$. Within the saturation approach, the gluon distribution presents a maximum at $k_\perp \simeq Q_s(x)$. The dipole cross section in coordinate space r for MPM model may be evaluated as [24]

$$\sigma_{\rm dip}(\tau_r) = \sigma_0\left(1 - \frac{2(\frac{\tau_r}{2})^\xi K_\xi(\tau_r)}{\Gamma(\xi)}\right), \tag{13}$$

where $\xi = 1 + \delta n$ and $\tau_r = rQ_s(x)$ is the scaling variable in the position space. Accordingly, the nuclear gluon distribution is obtained from Eqs. (11) and (12). The same procedure has been applied to the IN and GBW models. Interestingly, as the hard scale associated to the process is $\mu^2 = m_Z^2$, one expects that small dipoles (large $k_\perp$ gluons) will be the dominant contribution to the cross section. This means that $\mu^2 \gg Q_{s,A}(x)^2$ and the nuclear shadowing should be quite small. A good approximation for the nuclear UGD would be $\mathcal{F}_A(x,k_\perp) \approx A\mathcal{F}_p(x,k_\perp)$.

Models for nuclear UGDs are very scarce in literature. It would be worth comparing the present calculations with the numerical results from nuclear UGDs evolved by DGLAP or Ciafaloni-Catani-Fiorani-Marchesini evolution equations as studied in Refs. [36–38]. The advantage would be the introduction of other effects as antishadowing and European Muon Collaboration effects. The models based on Glauber-Gribov formalism bring only information on the shadowing effects to the referred process. Another source of theoretical uncertainty is the treatment for the skewedness correction once the effect is enhanced in the production amplitude squared.

III. NUMERICAL RESULTS AND DISCUSSION

Let us start by presenting the results for the Z^0 photoproduction in γp scattering. The corresponding energies for the ep colliders are exhibited in Table I. In Fig. 1 the predictions for the IN (dotted curve), MPM (dashed curve) and GBW (dot-dashed curve) models are shown as a function of photon-proton center of mass energy, $W_{\gamma p}$. In the TeV energy scale the cross section has the order of magnitude of $\sigma(\gamma^* p \to Z^0 p) \approx 0.1$ pb and a large theoretical uncertainty. Accordingly, the GBW model gives a lower bound for the cross section values and weaker energy behavior compared to MPM and IN. The reason is the DGLAP-like evolution embedded in both IN and MPM models for the UGD. The x value probed at $W_{\gamma p} = 1$ TeV is $\sim 10^{-3}$. The output coming from the MPM model can be parametrized in the following way: $\sigma_{\rm MPM}(\gamma p \to Z^0 p) = [180\ {\rm fb}](W_{\gamma p}/W_0)^{1.13}$ (with $W_0 = 10^3$ GeV). Notice that

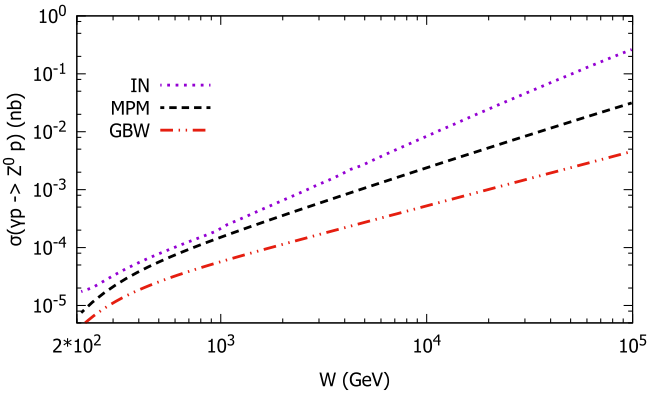

FIG. 1. Cross section $\sigma(\gamma^* p \to Z^0 p)$ as a function of photon-proton center of mass energy, $W_{\gamma p}$. Numerical results for IN, MPM, and GBW phenomenological models are presented.

the prediction from Ref. [12] is properly reproduced here by using the Ivanov-Nikolaev UGD. A steeper growth is predicted by Motyka and Watt (MW) in Ref. [11], where the color dipole picture is considered and by using the impact parameter saturation model (IP-SAT) and time-like Z^0 boson. The IP-SAT parametrization includes DGLAP evolution for the dipole cross section and the result scales as $\sigma_{\rm MW}(\gamma p \to Z^0 p) = [37\ {\rm fb}](W_{\gamma p}/W_0)^{1.73}$, with $W_0 = 1.3 \times 10^3$ GeV.

The analyses for nuclear targets are presented in Fig. 2. Predictions from the three phenomenological models are shown for the nuclear species presented in Table II and for proton as a baseline. As examples of order of magnitude one has $\sigma(\gamma Pb \to Z^0 Pb) \approx 84.6(260)$ pb and $\sigma(\gamma O \to Z^0 O) \approx 2.46(8.3)$ pb at HL-LHC(FCC) energy. The dependence on atomic mass number from MPM model (for $A > 1$) is given by $\sigma^{\gamma A}_{\rm MPM} = \sigma_A A^\delta$, where $\sigma_A = 50.5$ fb and $\delta = 1.39$ at the HL-LHC and $\sigma_A = 216$ fb and $\delta = 1.33$ at the FCC. This result is consistent with the weak absorption limit for the nuclear dipole cross section typical for Z^0 production. In the figure the predictions are shown for $W^{\rm max}_{\gamma A} = \sqrt{s_{eA}}$.

In Table III the cross section times branching ratio into dileptons (in units of fb) is presented for ep and eA collisions. Here, the interest is in very small $Q^2 \ll 1$ GeV^2 range where the photoproduction cross section is independent of photon virtuality. Therefore, the $ep(A) \to eZ^0 p(A)$ cross section can be written as

$$\frac{d\sigma}{dW^2} = \frac{\alpha_{em}}{2\pi s}\left[\frac{1+(1-y)^2}{y}\ln\frac{Q^2_{\rm max}}{Q^2_{\rm min}} - \frac{2(1-y)}{y}\left(1 - \frac{Q^2_{\rm min}}{Q^2_{\rm max}}\right)\right] \times \sigma^{\gamma p(A)}(W^2), \tag{14}$$

where y is the inelasticity variable and $Q^2_{\rm min} = m_e^2 y^2/(1-y)$. The corresponding number of events per year is also presented. The run with oxygen is comparable in number of events for the proton target. The experimental feasibility is enhanced in eA case compared to the ep machine. This is

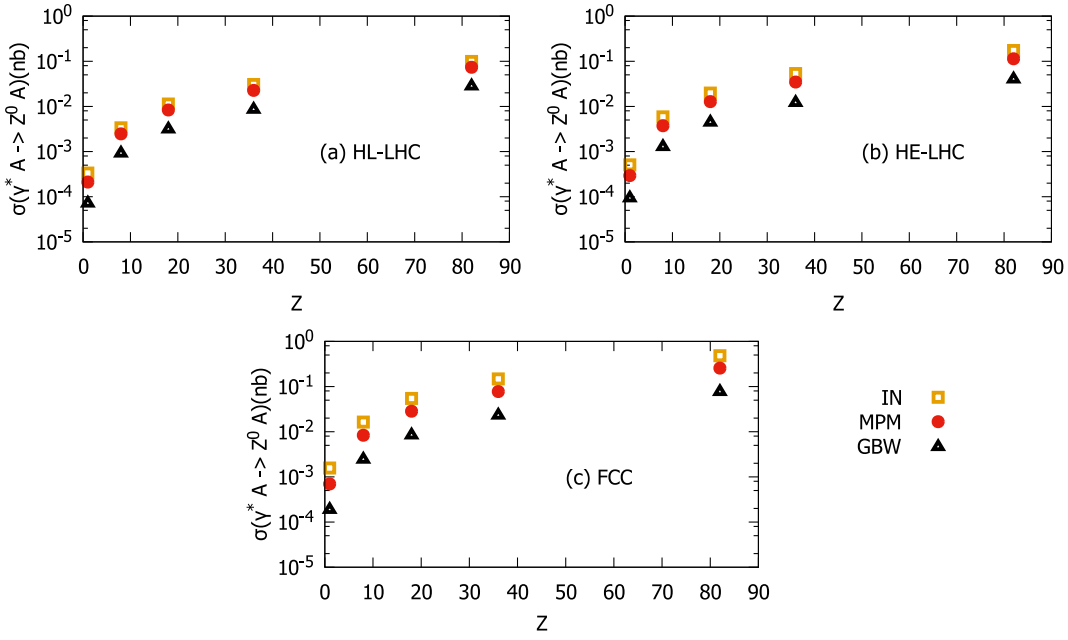

FIG. 2. Cross section $\sigma(\gamma^* p(A) \to Z^0 p(A))$ as a function of atomic number Z at the energies of (a) HL-LHC, (b) HE-LHC, and (c) FCC. The predictions from IN, MPM, and GBW models are shown for O, Ar, Kr, Pb nuclei and proton as well. The corresponding energies are presented in Table II.

specially important when kinematic cuts are imposed in order to remove the main dilepton QED background. The predictions considering the decay into hadrons is larger by a factor 20 but the experimental feasibility worsens.

Let us now move to ultraperipheral collisions. The cross section to produce a Z^0 boson in a proton-proton collision within the Weizsäcker-Williams approximation is given by [39–41]

$$\sigma(pp \to pp + Z^0) = 2 \int_0^\infty \frac{dn_\gamma^p}{d\omega} \sigma(\gamma + p \to Z^0 + p) d\omega,$$

where ω is the photon energy and $dn_\gamma^p/d\omega$ is the photon spectrum for protons. In the numerical calculations we have used the photon spectrum from Ref. [42]. The corresponding rapidity distribution is obtained as follows:

$$\frac{\sigma(pp \to pp + Z^0 p)}{dy} = \omega \frac{dn_\gamma^p}{d\omega} \sigma_{\gamma+p \to Z^0+p}(\omega), \quad (15)$$

in which the rapidity y of the produced Z^0 state with mass M_Z is related to the photon energy through $y = \ln(2\omega/M_Z)$. The rapidity distributions are shown in Fig. 3 and the calculations are for collision energies of (a) the HL-LHC, (b) HE-LHC, and (c) FCC colliders. The dotted, dashed, and dot-dashed curves are the results for the IN, MPM, and GBW UGDs, respectively. Here, the predictions are presented without absorption effects which depend on the rapidity. For instance, the absorptive correction at 14 TeV for $y = 0$ is $\langle S^2 \rangle \simeq 0.8$ whereas it is $\langle S^2 \rangle \simeq 0.6$ for $y = 2$ [12]. The theoretical uncertainty is still sizable. At the energy of HL-LHC, our predictions are in agreement with those in Refs. [11–13]. In general, the numerical results obtained using k_T-factorization approach are higher than those from color dipole framework. The rapidity distribution for higher hadron energies (HE-LHC and FCC) can be directly compared with the results of Ref. [13]. There, two dipole cross section have been considered (bCGC and IP-SAT models) within the color dipole picture. The order of magnitude of the cross sections are in agreement. The experimental feasibility is promising by using the dilepton decay channel. A careful analysis by

TABLE III. Cross section in units of fb and event rates/year times branching ratio for exclusive Z^0 photoproduction in ep and eA collisions. The results are presented for the MPM UGD model as a baseline. Numerical calculation are presented for O and Pb nuclei.

Collider	Nucleus	$\sigma_{ep(A)}$ (fb)	Number of events per year
HL-LHC	p	7.11	60.6
	O	70.3	3.28
	Pb	1.97×10^3	7.07
HE-LHC	p	10.9	140
	O	113	13.69
	Pb	3.27×10^3	30.09
FCC	p	30.9	494
	O	349	125.62
	Pb	1.04×10^4	287.98

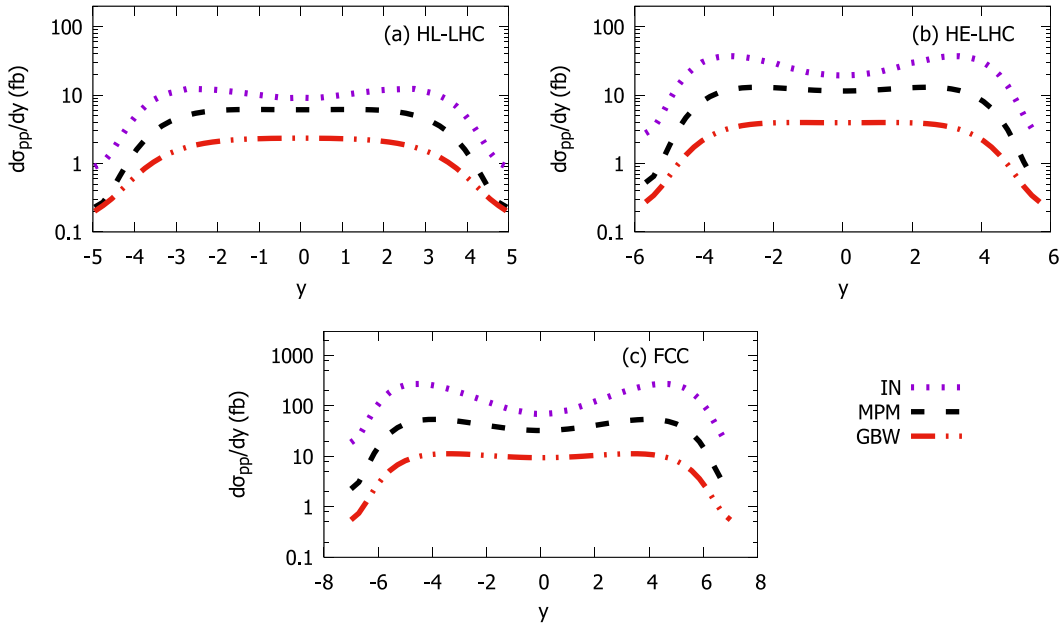

FIG. 3. Rapidity distribution for exclusive Z^0 production in pp collisions. Predictions are shown for the energies of (a) HL-LHC, (b) HE-LHC, and (c) FCC.

using kinematic cuts should remove the large background coming from $\gamma\gamma \to \ell^+\ell^-$ process. The search for exclusive Z^0 production in proton-proton collisions can follow similar methodology employed in the corresponding search in $p\bar{p}$ collisions at Tevatron energies [5].

Finally, the Z^0 exclusive production is investigated in ultraperipheral heavy ion collisions (UPCs). The corresponding rapidity distribution for the coherent production is given by [43]

$$\frac{\sigma(AA \to AZ^0A)}{dy} = \omega \frac{dn_\gamma^A}{d\omega} \sigma_{\gamma+A\to Z^0+A}(\omega), \qquad (16)$$

where $dn_\gamma^A/d\omega$ is the photon spectrum for nuclei. The analytical photon flux for $b > 2R_A$ has been used in [39]. In Fig. 4 the rapidity distribution is shown for oxygen (O) and lead (Pb) nuclei: upper and lower plots, respectively. This is presented for the energies of HL-LHC and FCC.

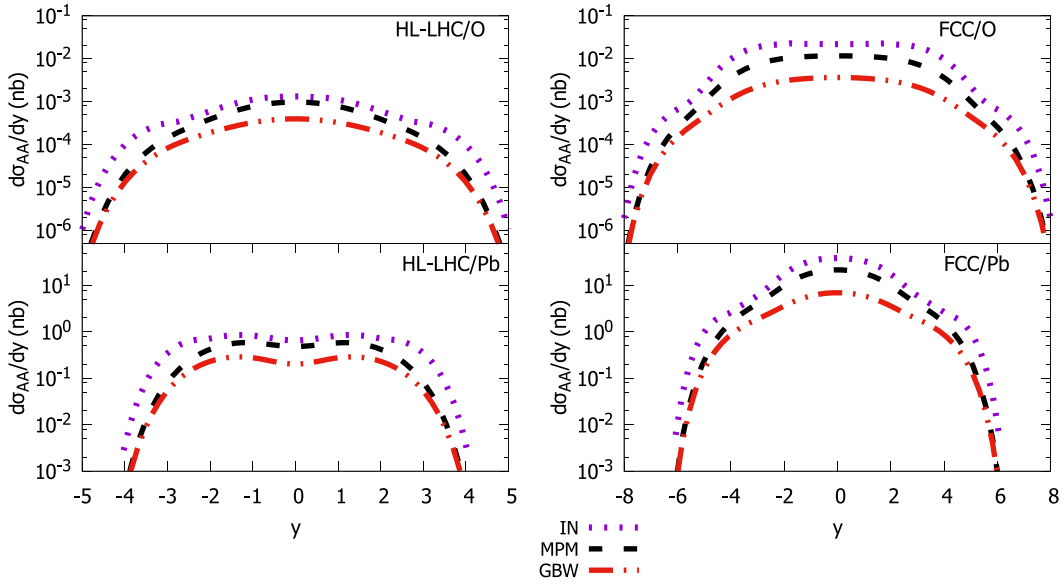

FIG. 4. Rapidity distribution for Z^0 production in AA collisions. Prediction are presented for oxygen (upper plots) and lead (lower plots) nuclei at the energies of HL-LHC (plots on the left) and FCC (plots on the right).

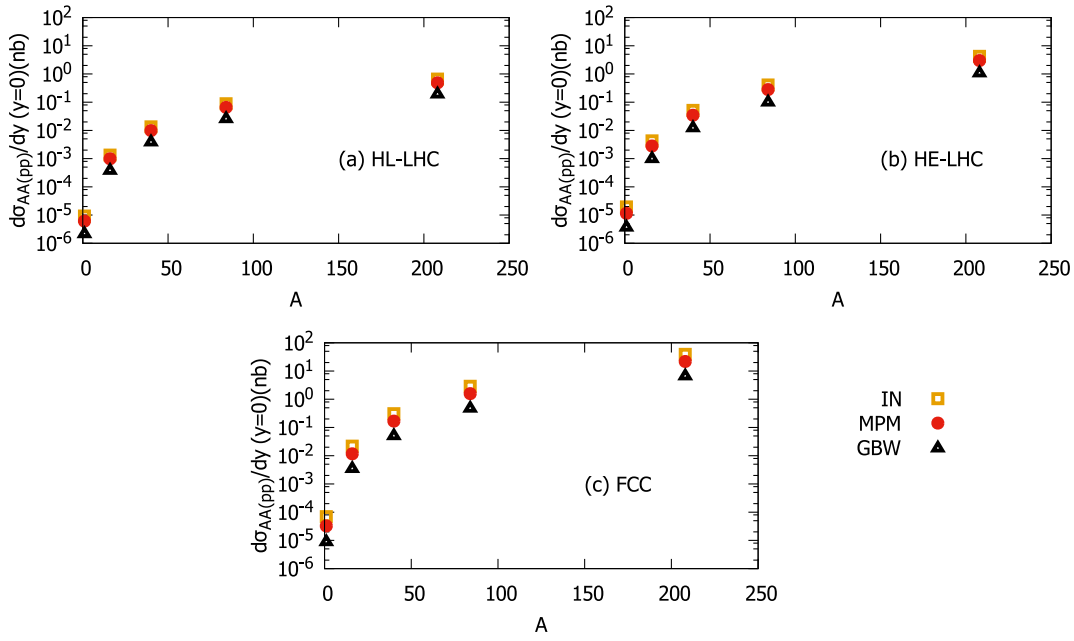

FIG. 5. Rapidity distribution for Z^0 production in AA collisions at mid-rapidity $y = 0$ as a function of the atomic mass number A. The predictions from IN, MPM and GBW models are shown for O, Ar, Kr, Pb nuclei and proton as well. Predictions are shown for the energies of (a) HL-LHC, (b) HE-LHC, and (c) FCC.

The predictions are somewhat larger than the ones presented in Ref. [13] where the color dipole approach is considered. There, $d\sigma_{AA}(y=0)/dy \simeq 0.6$ nb in contrast with present calculation $d\sigma_{AA}(y=0)/dy \simeq 10$ nb. In both approaches the theoretical uncertainty is large, specially that one associated with the specific model for the dipole cross section or UGD.

In Fig. 5 the predictions for rapidity distributions at midrapidity, $y = 0$, are shown for the nuclear species presented in Table II as well as for protons. The cross sections are exhibited as a function of the atomic mass number A for the energies of (a) HL-LHC, (b) HE-LHC, and (c) FCC. The predictions for MPM and IN models are quite similar at this scale and a lower bound is given by the GBW model.

In order to summarize the results for pp and PbPb collisions in Table IV the event rates/year are presented, where the production cross section has been multiplied by branching ratio for decays into dileptons. Two rapidity ranges are considered: $|y| \leq 2$ (central rapidities) and $+2.0 \leq y \leq +4.5$. (forward rapidities). Results are presented for the MPM UGD model as a representative example of application. The present calculation is more comprehensive than those in Ref. [13] since light nuclei are also taken into account.

IV. CONCLUSIONS

In this work the exclusive production of Z^0 boson is investigated in ep and eA collisions within the k_T-factorization formalism. The theoretical uncertainty is studied by comparing the results for different unintegrated gluon distributions available in literature. It was found that the corresponding variance is large when models containing parton saturation effects are contrasted to those where they are not applied. The analysis is done in the kinematic range of interest of EIC and the LHeC. As a byproduct the Z^0 photoproduction is also investigated in pp and AA

TABLE IV. The event rates/year for exclusive Z^0 photoproduction in pp and PbPb collisions in different rapidity ranges. The results are presented for the MPM UGD model as a baseline.

	pp collisions		*PbPb collisions*	
Collider	$-2.0 < y < +2.0$	$+2.0 < y < +4.5$	$-2.0 < y < +2.0$	$+2.0 < y < +4.5$
HL-LHC	1.39×10^3	531	364	45.8
HE-LHC	8.15×10^3	461	1.33×10^3	183
FCC	7.54×10^3	6.60×10^4	5.92×10^4	8.31×10^3

collisions. The application was restricted to the coherent scattering and predictions for incoherent scattering would be valuable. A comprehensive study is done concerning different nuclear species relevant for the LHC future runs. The experimental measurement feasibility is briefly discussed.

ACKNOWLEDGMENTS

This work was financed by the Brazilian funding agency CNPq. We are thankful to Krzysztof Piotrzkowski (Université Catholique de Louvain) for his contribution in this paper.

[1] J. Berryhill and A. Oh, J. Phys. G **44**, 023001 (2017).
[2] R. Chislett, Studies of hadronic decays of high transverse momentum W and Z bosons with the ATLAS detector at the LHC, Ph.D. thesis, University College London, 2014.
[3] M. G. Albrow, T. D. Coughlin, and J. R. Forshaw, Prog. Part. Nucl. Phys. **65**, 149 (2010).
[4] L. A. Harland-Lang, V. A. Khoze, and M. G. Ryskin, Eur. Phys. J. C **76**, 9 (2016).
[5] T. Aaltonen *et al.* (CDF Collaboration), Phys. Rev. Lett. **102**, 222002 (2009).
[6] M. Medina Jaime, Produção exclusiva de bósons Z em colisões pp no experimento CMS/LHC, Ph. D. thesis, Campinas State Universiy, 2015.
[7] M. Hentschinski *et al.*, arXiv:2203.08129.
[8] J. Bartels and M. Loewe, Z. Phys. C **12**, 263 (1982).
[9] J. Pumplin, arXiv:hep-ph/9612356.
[10] V. P. Goncalves and M. V. T. Machado, Eur. Phys. J. C **56**, 33 (2008); **61**, 351(E) (2009).
[11] L. Motyka and G. Watt, Phys. Rev. D **78**, 014023 (2008).
[12] A. Cisek, W. Schafer, and A. Szczurek, Phys. Rev. D **80**, 074013 (2009).
[13] R. Coelho and V. Gonçalves, Nucl. Phys. **B956**, 115013 (2020).
[14] J. L. Abelleira Fernandez *et al.* (LHeC Study Group Collaboration), J. Phys. G **39**, 075001 (2012).
[15] P. Agostini *et al.* (LHeC, FCC-he Study Group Collaborations), J. Phys. G **48**, 110501 (2021).
[16] K. D. J. André *et al.*, Eur. Phys. J. C **82**, 40 (2022).
[17] A. Abada *et al.* (FCC Collaboration), Eur. Phys. J. C **79**, 474 (2019).
[18] A. Abada *et al.* (FCC Collaboration), Eur. Phys. J. Special Topics **228**, 755 (2019).
[19] G. M. Peccini, L. S. Moriggi, and M. V. T. Machado, Phys. Rev. D **102**, 094015 (2020).
[20] G. M. Peccini, L. S. Moriggi, and M. V. T. Machado, Phys. Rev. D **103**, 054009 (2021).
[21] W. Schafer, G. Slipek, and A. Szczurek, Phys. Lett. B **688**, 185 (2010).
[22] L. S. Moriggi, G. M. Peccini, and M. V. T. Machado, Phys. Rev. D **103**, 034025 (2021).
[23] P. Agostini *et al.* (LHeC, FCC-he Study Group Collaborations), J. Phys. G **48**, 110501 (2021).
[24] L. Moriggi, G. Peccini, and M. Machado, Phys. Rev. D **102**, 034016 (2020).
[25] I. Ivanov and N. N. Nikolaev, Phys. Rev. D **65**, 054004 (2002).
[26] K. J. Golec-Biernat and M. Wusthoff, Phys. Rev. D **59**, 014017 (1998).
[27] K. Golec-Biernat and S. Sapeta, J. High Energy Phys. 03 (2018) 102.
[28] K. T. R. Davies and J. R. Nix, Phys. Rev. C **14**, 1977 (1976).
[29] Z. Citron *et al.*, CERN Yellow Rep. Monogr. **7**, 1159 (2019).
[30] F. Bordry *et al.*, arXiv:1810.13022.
[31] S. Amoroso *et al.*, arXiv:2203.13923.
[32] V. N. Gribov, Sov. Phys. JETP **29**, 483 (1969), http://www.jetp.ras.ru/cgi-bin/e/index/r/56/3/p892?a=list.
[33] V. N. Gribov, Zh. Eksp. Teor. Fiz. **57**, 1306 (1969), http://jetp.ras.ru/cgi-bin/dn/e_030_04_0709.pdf.
[34] N. Armesto, Eur. Phys. J. C **26**, 35 (2002).
[35] H. De Vries, C. De Jager, and C. De Vries, At. Data Nucl. Data Tables **36**, 495 (1987).
[36] E. de Oliveira, A. Martin, F. Navarra, and M. Ryskin, J. High Energy Phys. 09 (2013) 158.
[37] M. Modarres and A. Hadian, Nucl. Phys. **A983**, 118 (2019).
[38] M. Modarres and A. Hadian, Phys. Rev. D **98**, 076001 (2018).
[39] S. Klein and J. Nystrand, Phys. Rev. C **60**, 014903 (1999).
[40] S. Klein and P. Steinberg, Annu. Rev. Nucl. Part. Sci. **70**, 323 (2020).
[41] S. R. Klein, J. Nystrand, J. Seger, Y. Gorbunov, and J. Butterworth, Comput. Phys. Commun. **212**, 258 (2017).
[42] M. Drees and D. Zeppenfeld, Phys. Rev. D **39**, 2536 (1989).
[43] C. A. Bertulani, S. R. Klein, and J. Nystrand, Annu. Rev. Nucl. Part. Sci. **55**, 271 (2005).